Appendix 1. Automated vascular segmentation

The vascular segmentation network we utilized was OCTA-Net[1]. This network consists of two phases: coarse and fine segmentation stages.

In the coarse stage, a split-based coarse segmentation (SCS) module is designed to produce preliminary pixel-level and centerline-level confidence maps. The SCS module is an encoder-decoder architecture with a partially shared encoder (with the first three encoder layers shared) and two decoder branches, a pixel-level vessel segmentation branch and a centerline-level vessel segmentation branch, to balance vessel information at both levels. Each encoder or decoder layer adopts ResNeSt[2] block with a split attention module. ResNeSt block regards a series of representations as a combination of different feature groups and then applies a channel attention mechanism to these feature groups. Mathematically, the coarse stage can be expressed as **Eq. 1**

$$\begin{cases} I_p = f_{pd}\left(f_e(I_{SVC+DVC})\right), \\ I_c = f_{cd}\left(f_e^3(I_{SVC+DVC})\right). \end{cases} \quad (1)$$

where $I_{(SVC+DVC)}$ represent the input *en face* image; f_e represents the partially shared encoder (the shared first three encoder layers are denoted as f_e^3); f_{pd} and f_{cd} represent the pixel-level and the centerline-level vessel segmentation branches; and their outputs are denoted as I_p and I_c respectively.

In the fine stage, a split-based refining segmentation (SRS) module is proposed to further fuse these vessel confidence maps to produce the final optimized results. In order to fully integrate pixel-level and centerline-level vessel information from the SCS module, the predicted pixel-level and centerline-level vessel maps and the original (single channel) OCT-A image are first concatenated as input (total 3 channels) to the SRS module. In addition, the SRS module will produce adaptive propagation coefficients to refine the pixel-level and centerline-level maps respectively. In the SRS module, a mini network including three convolutional layers with kernels of 3 × 3 is designed to refine the pixel-level map from the coarse stage. Besides, one additional 3 × 3 convolutional layer is appended to the second layer of the mini network to refine the centerline-level map from the coarse stage. Finally, the refined pixel- and centerline-level maps are then merged into a complete vessel segmentation map, by choosing the larger value from the two maps at each pixel. The fine stage can be formulated as **Eq. 2**

$$\begin{cases} \widetilde{I_p} = f_{pw}\left(I_{SVC+DVC}, I_p, I_c\right) * I_p, \\ \widetilde{I_c} = f_{cw}\left(I_{SVC+DVC}, I_p, I_c\right) * I_c, \\ I_f = max\left(\widetilde{I_p}, \widetilde{I_c}\right). \end{cases} \quad (2)$$

where $f_{pw}(\cdot)$ and $f_{cw}(\cdot)$ produce adaptive propagation coefficients to refine the pixel-level and centerline-level maps respectively; $*$ represents the operation of adaptive aggregation to obtain the refined pixel-level result $\widetilde{I_p}$ and centerline-level $\widetilde{I_c}$; I_f is the refined complete vessel segmentation map

obtained by choosing the maximum between $\widetilde{I_p}$ and $\widetilde{I_c}$ at each pixel.

Appendix 2. Automated FAZ segmentation

In this study, we also employed a novel FAZ segmentation network[3]. This model consists of three encoders as shown in **Appendix Figure 1**, a voting gate module and a FAZ segmentation head. In their method, the ResNet-50[4] was employed as feature encoder, where the first 7 × 7 convolution layer is replaced by 3 × 3 convolution with the same padding, which ensures that the input size of the gate block is consistent with the size of the image. In their implementation, three encoders share weights except the first convolutional block to limit the number of learnable parameters. In order to ensure the parameter diversity of different encoders, different parameter initialization strategies was adapted for the first convolutional block of different encoders, namely random initialization, Xavier initialization[5] and He initialization.[6]

The voting gate module consists of multiple 3 × 3 convolutional layers with batch normalization (BN) and ReLU activation. The last layer is a softmax layer. The gate module can learn to dynamically select features from two folds: features of different encoders and features of different spatial locations in an encoder. The process can be formulated as **Eq. 3**

$$Y = \sum_{i=1}^{n} G_i(x) \circ E_i(x), \qquad (3)$$

where $\sum_{i=1}^{n} G_i(x)=1$ and $G_i(x)$, the i_{th} logit of the output of gate module $G(x)$, indicates the voting weight for encoder E_i. '$\circ$' denotes element-wise multiplication, n is the number of the encoders and x is the input. The segmentation head is a multiple convolutional block to obtain the probability map of FAZ. Example results of FAZ segmentation was shown in **Appendix Figure 2**

Appendix 3. Vascular orientation distribution

Vascular orientation distribution (VOD) was represented as the direction histogram in polar coordinates, where the direction of each vascular pixel is calculated by using the hessian matrix. In this paper, the multi-scale hessian algorithm[7] was applied to detect the direction of vascular with various widths. As shown in **Appendix Figure 3**, the direction of each vascular pixel is represented as an angle from 0 to 180 degrees. In order to meet the angle range in polar coordinates, we expand the angle of each pixel to twice the original. Then, a polar plot of orientation distribution was generated to show the number of the pixel at each angle from 0 to 360 degrees. This orientation distribution curve exhibits the unique pattern of the vasculature map in the OCTA. Quantitative measures of the vessel orientation pattern can be achieved by analyzing the polar plot region encompassed by the orientation distribution curve. According to the observation that the orientation pattern for the OCTA vascular depicts a roughly elliptical shape, the ellipse fitting method proposed

in[8] was utilized to estimate the general equation of the ellipse and then the major axis and a minor axis were calculated through the fitting result. Finally, the VOD was represented as the ratio of lengths between the major axis and minor axis. The VOD is a representation of vessel anisotropy, a larger VOD indicates that the flow of the vascular tends to be consistent and there are fewer curves on the vascular, vice versa.

References

1. Ma Yuhui, Hao Huaying, Xie Jianyang, et al. ROSE: A Retinal OCT-Angiography Vessel Segmentation Dataset and New Model. IEEE Transactions on Medical Imaging. 2020.
2. Zhang, H., Wu, C., Zhang, Z., Zhu, Y., Zhang, Z., Lin, H., Sun, Y., He, T., Mueller, J., Manmatha, R., Li, M., Smola, A.: Resnest: Split-attention networks. arXiv (2020)
3. Hao Jinkui, Shen Ting, Zhu, Xueli, et al. Retinal Structure Detection in OCTA Image via Voting-based Multi-task Learning, 10.48550/ARXIV.2208.10745, 2022.
4. He, K., Zhang, X., Ren, S., Sun, J.: Deep residual learning for image recognition. In: Proceedings of the IEEE Conference on Computer Vision and Pattern Recognition, pp. 770–778 (2016)
5. Glorot, X., Bengio, Y.: Understanding the difficulty of training deep

feedforward neural networks. In: Proceedings of the Thirteenth International Conference on Artificial Intelligence and Statistics, pp. 249–256 (2010). JMLR Workshop and Conference Proceedings

6. He, K., Zhang, X., Ren, S., Sun, J.: Delving deep into rectifiers: Surpassing human-level performance on imagenet classification. In: Proceedings of the IEEE International Conference on Computer Vision, pp. 1026–1034 (2015)

7. Jerman, T., Pernuˇs, F., Likar, B., Sˇpiclin, : Enhancement of vascular structures in 3d and 2d angiographic images. IEEE Transactions on Medical Imaging 35(9), 2107–2118 (2016). doi:10.1109/TMI.2016.2550102

8. Szpak, Z.L., Chojnacki, W., van den Hengel, A.: Guaranteed ellipse fitting with the sampson distanc. ECCV 2012, 87–100 (2012)

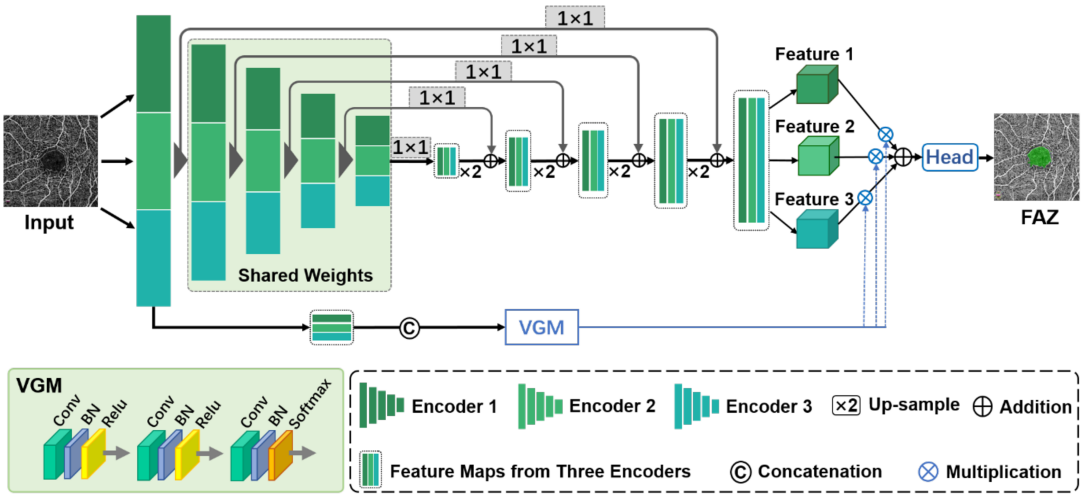

Appendix Figure 1 Architecture of the proposed FAZ segmentation network.

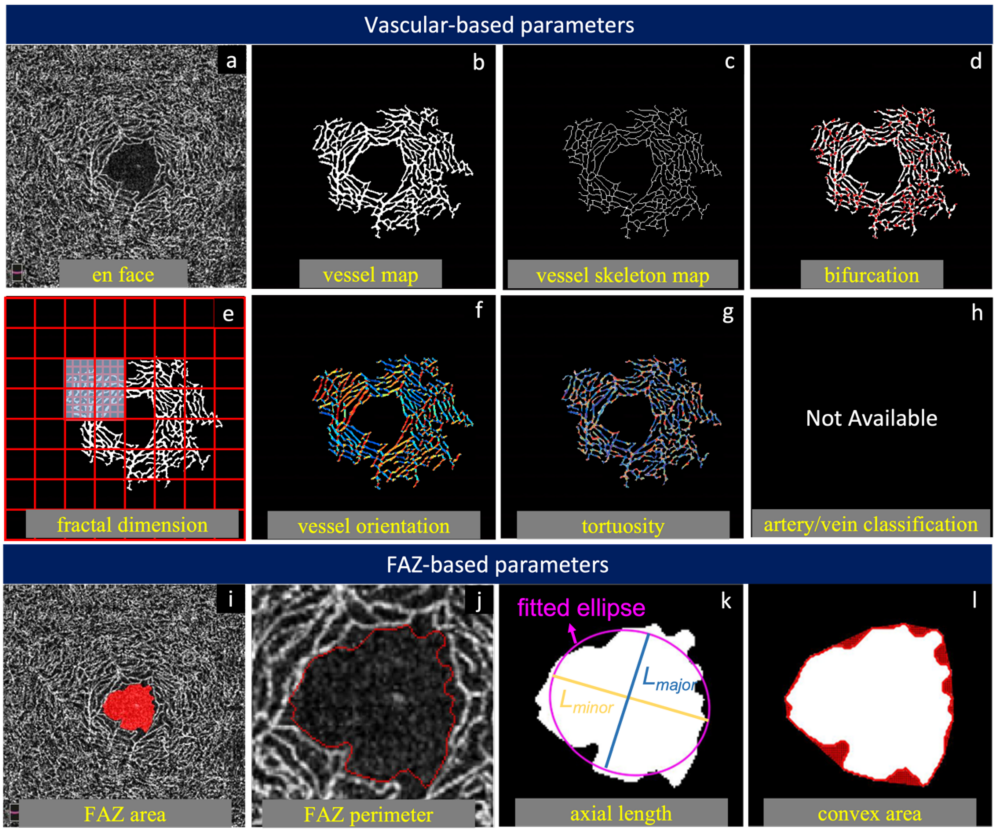

Appendix Figure 2(a), The OCTA metric for deep vascular complexes, (a) shows a 3 × 3 mm^2 *en face* DVC angiogram. (b) and (c) show the automated segmented vessel map and vessel skeleton map of (a), respectively. By calculating the ratio of vasculatures in (b) and (c), vascular area density (VAD) and vascular length density (VLD) can be derived, respectively. The red dots in (d) indicate the vascular bifurcations (VB). (e)-(h) illustrate vascular fractal dimension (VFD), vascular orientation distribution (VOD), vascular tortuosity (VT), and arterioles/venules (AV) classification, respectively. (Note: the AV classification is only applied to the 6 × 6 mm^2 *en face* angiogram in this work) (i) is the detected FAZ area (FA), and (j) shows its perimeter (FP). The Circularity of the FAZ (FC) is calculated as: $FC = 4\pi * FA/FP^2$. (k) shows the major and minor axes of the fitted ellipse of the FAZ. The axis ratio of the FAZ (FAR) is defined as the ratio between major axial length L_{major} and minor axial length L_{minor}, while the roundness of the FAZ (FR) is calculated via $FR = 4\pi * FA/L^2$. (l) shows the convex area of the FAZ, and the solidity of the FAZ (FS) is defined as the ratio between the FA and the convex area.

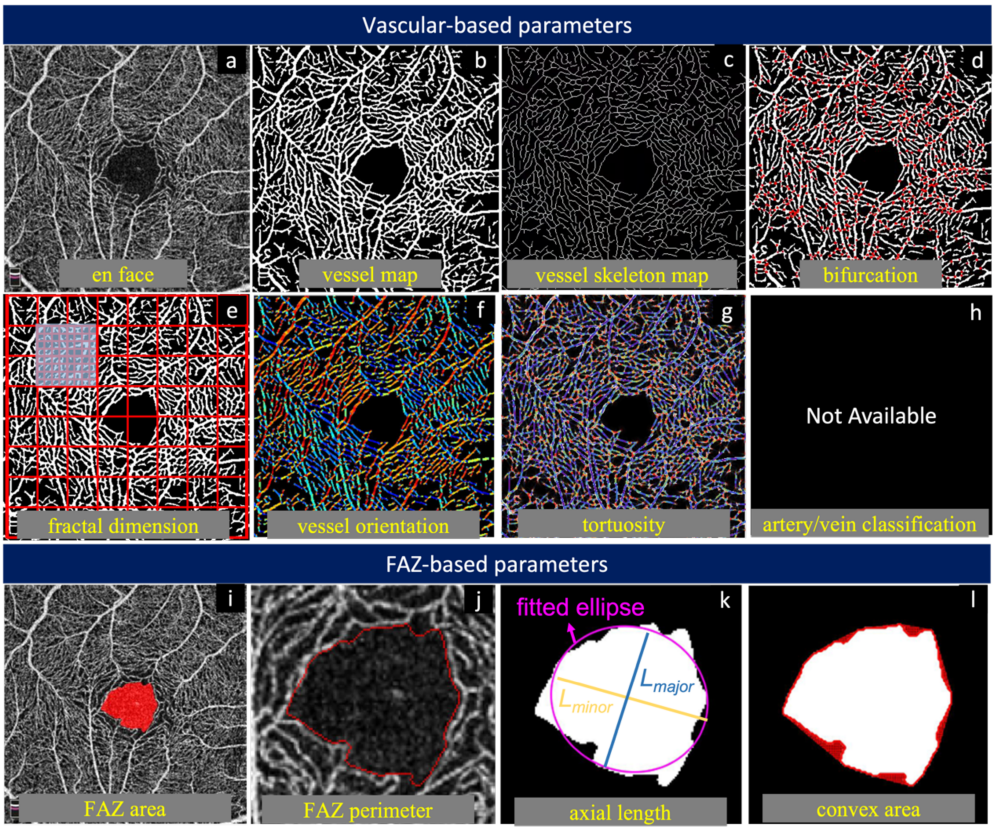

Appendix Figure 2(b), The OCTA metric for inner vascular complexes, (a) shows a 3 × 3 mm^2 *en face* IVC angiogram. (b) and (c) show the automated segmented vessel map and vessel skeleton map of (a), respectively. By calculating the ratio of vasculatures in (b) and (c), vascular area density (VAD) and vascular length density (VLD) can be derived, respectively. The red dots in (d) indicate the vascular bifurcations (VB). (e)-(h) illustrate vascular fractal dimension (VFD), vascular orientation distribution (VOD), vascular tortuosity (VT), and arterioles/venules (AV) classification, respectively. (Note: the AV classification is only applied to the 6 × 6 mm^2 *en face* angiogram in this work.) (i) is the detected FAZ area (FA), and (j) shows its perimeter (FP). The Circularity of the FAZ (FC) is calculated as: $FC = 4\pi * FA/FP^2$. (k) shows the major and minor axes of the fitted ellipse of the FAZ. The axis ratio of the FAZ (FAR) is defined as the ratio between major axial length L_{major} and minor axial length L_{minor}, while the roundness of the FAZ (FR) is calculated via $FR = 4\pi * FA/L^2$. (l) shows the convex area of the FAZ, and the solidity of the FAZ (FS) is defined as the ratio between the FA and the convex area.

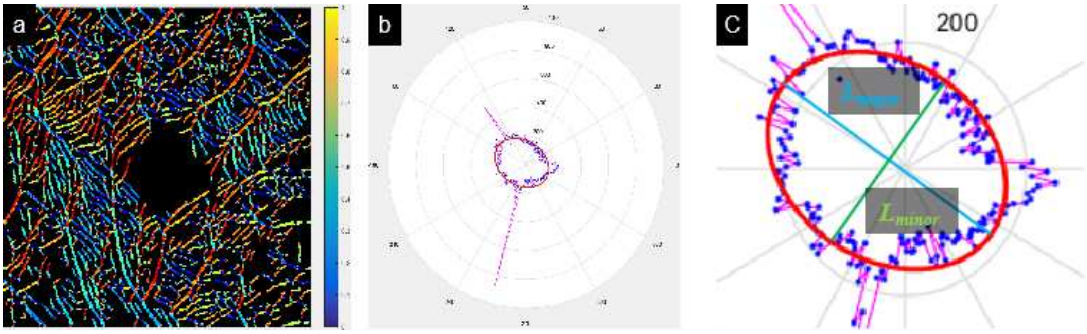

Appendix Figure 3 (a) is a color encoded map describing the vascular orientation distribution of the OCTA image, where similar colors indicate similar blood flow directions. **(b)** is a polar plot which shows the number of vascular pixels in (a) from 0 of 360 degrees based on their directions. **(c)** Illustrates the fitted ellipse of the orientation distribution points, and draws the major and minor axis.